ChemBioChem

Research Article
doi.org/10.1002/cbic.202400831

Chemistry Europe
European Chemical Societies Publishing

www.chembiochem.org

Proteomic Profiling of Potential E6AP Substrates via Ubiquitin-based Photo-Crosslinking Assisted Affinity Enrichment

Julian Schuck,[a] Christine Bernecker,[a] Martin Scheffner,[a] and Andreas Marx*[a]

The ubiquitin (Ub) ligase E6AP, encoded by the *UBE3A* gene, has been causally associated with human diseases including cervical cancer and Angelman syndrome, a neurodevelopmental disorder. Yet, our knowledge about disease-relevant substrates of E6AP is still limited, presumably because at least some of these interactions are rather transient, a phenomenon observed for many enzyme-substrate interactions. Here, we introduce a novel approach to trap such potential transient interactions by combining a stable E6AP-Ub conjugate mimicking the active state of this enzyme with photo-crosslinking (PCL) followed by affinity enrichment coupled to mass spectrometry (AE-MS). To enable PCL, we equipped Ub with diazirine moieties at distinct positions. We validated our PCL assisted AE-MS approach by identification of known (e.g. PSMD4, UCHL5) and potential new (e.g. MSH2) substrates of E6AP. Our findings suggest that PCL assisted AE-MS is indeed suited to identify substrates of E6AP, thereby providing insights into E6AP-associated pathologies, and, potentially, of other enzymes of the Ub-conjugating system.

Introduction

E6AP, which is encoded by the *UBE3A* gene,[1] is the founding member of the HECT family of E3 ubiquitin (Ub) ligases.[2] E3 ligases are mainly responsible for the substrate specificity of the Ub-conjugation system.[3] Thus, elucidation of the respective substrate pattern provides intimate insights into the cellular processes and pathways a given E3 is involved in. Remarkably, dysregulation of E6AP has been causally associated with three different clinical pictures. In complex with the E6 oncoprotein of HPVs, it targets the tumor suppressor p53 as well as other cellular proteins for ubiquitination and subsequent proteasomal degradation, thereby contributing to cervical carcinogenesis.[4] Genetic aberrations of the *UBE3A* gene resulting in loss of a functional E6AP protein are the cause of Angelman syndrome (AS), a neurodevelopmental disorder, while amplification of the *UBE3A* gene, potentially resulting in E6AP overexpression, results in Dup15q syndrome, another neurodevelopmental disorder.[5] In addition, there is evidence to suggest that also in the absence of HPVs, E6AP may be involved in the development of solid cancers including breast and prostate cancers.[6]

In contrast to cervical carcinogenesis, only little is known about the substrates and interaction partners of E6AP that are relevant for the development of AS and/or the Dup15q syndrome.[7] Various approaches including proximity-based approaches such as coprecipitation analysis,[8] proteomics analysis of AS mouse models,[9] and orthogonal ubiquitin-based approaches to directly identify potential substrates[10] have been employed to elucidate the interactome and ubiquitome, respectively, of E6AP. Although this resulted in the identification of a number of interesting candidates including HHR23A,[11] RING1B,[12] HERC2,[13] NEURL4,[8a] PMRT5,[10] and TKT1,[9] the pathophysiological relevance of these interactions remains to be proven. In addition, the approaches used so far have limitations. For instance, substrates that transiently or weakly interact with E6AP, a situation that holds true for many substrate-enzyme interactions, will not be identified by conventional coprecipitation analyses. Similarly, in comparative proteomics analyses of whole cells or tissues, it is not possible to distinguish between direct substrates of E6AP and proteins, whose ubiquitination status is indirectly affected by E6AP.

Unlike RING E3 ligases, which constitute the largest E3 family, HECT E3s as well as RBR E3s are "true" enzymes.[3] An essential intermediate step in E6AP-mediated ubiquitination is a transthiolation reaction, in which an activated Ub molecule is transferred from the cognate E2 enzyme (UbcH5, UbcH7) to the catalytic cysteine residue of E6AP.[2a] E6AP itself then catalyzes the covalent attachment of Ub to substrate proteins via isopeptide bond formation. Since substrates have to come into close proximity to the catalytic center of E6AP for isopeptide bond formation, we reasoned that stable E6AP-Ub conjugates mimicking the active E6AP-Ub thioester complex should be most suited for proximity-based identification of substrate proteins. This proposition is supported by recent structural studies revealing that E6AP adopts distinct conformational

[a] *J. Schuck, C. Bernecker, M. Scheffner, A. Marx*
Departments of Biology and Chemistry
Konstanz Research School Chemical Biology
University of Konstanz
Universitätsstraße 10, 78467 Konstanz (Germany)
E-mail: andreas.marx@uni-konstanz.de

Supporting information for this article is available on the WWW under https://doi.org/10.1002/cbic.202400831

states, specifically an "acceptor" state and, more importantly, a "donor" state, during the Ub transfer process.[14] The conformational plasticity observed between these two states underscores the dynamic nature of E6AP-substrate interactions and reinforces the potential of using E6AP-Ub conjugates to capture substrates that otherwise would not or only transiently interact with E6AP. To further increase the chances to identify transiently interacting substrates, we generated stable conjugates of E6AP with a Ub variant that harbors photo-reactive groups at distinct positions to enable covalent trapping of substrate proteins. Photo-crosslinking assisted affinity enrichment coupled to mass spectrometry (PCL-AE-MS) experiments with a respective E6AP-Ub conjugate indicate the applicability of our approach.

Results and Discussion

Generation of Ub Variants for Photo-crosslinking

To equip Ub with a photo-reactive group, we employed Ub variants that carry Cys residues at distinct positions. The introduced thiol groups serve as nucleophiles enabling the modification of Ub by Michael addition (Figure 1A). Based on an AlphaFold-generated model of Ub bound to the HECT domain of E6AP (Figure 1B),[15] we produced a Ub variant, in which S20, E24, and A46 were replaced by C (Ub-3C), and three variants, in which either S20, E24 or A46 were replaced by C. The criteria for selecting these residues were (i) even distribution on Ub surface, (ii) orientation facing away from the HECT domain to avoid potential crosslinking with the HECT domain, and (iii) side chain accessibility.

As photo-reactive probe we used 2-(3-methyl-3H-diazirine-3-yl)ethyl acrylate (DEA). For DEA synthesis (Figure S1), the diazirine moiety was introduced into 4-hydroxy-2-butanone according to Chou et al.[16] Subsequently, the acrylic functionality was added by EDC-catalyzed ester coupling with acrylic acid. Finally, the resulting DEA probe was coupled to the aforementioned Ub variants via Michael addition. Monitoring of the reaction products by ESI-MS/TOF measurements at different times demonstrated a rapid reaction with almost quantitative conversion after 5 min (shown in Figure 1C for Ub-3C). The reaction was also monitored by fluorescein-5-maleimide labeling of unreacted thiol groups,[17] again showing the high efficiency of the labeling reaction (Figure S2). With increasing reaction time, a small fraction of Ub-3C is modified with a forth DEA moiety (Figure 1C), potentially resulting from unspecific labelling of nucleophilic amino acid side chains. Thus, we concluded that a reaction time of 5 min is sufficient for efficient and site-specific labeling of Ub with the DEA probe.

To determine, if DEA-modified Ub variants can in general be applied to monitor the interaction of Ub with other proteins, we resorted to Ub variants carrying a DEA moiety at position 20 (Ub C20), 24 (Ub C24), or 46 (Ub C46) or at all three positions (Ub C3x). The DEA-modified Ub variants were incubated with known Ub binding proteins (NDP52, OTUB1).[18] After 3 h, PCL was performed at 365 nm (2.4 J/cm^2). In case of successful crosslinking, the respective Ub binding protein should experience a molecular mass shift of approximately 10 kDa (Figure 2A). Indeed, such an increase was observed for both NDP52 and OTUB1 with Ub C46 and Ub-3DEA, but not or with very low efficiency with Ub C20 and Ub C24 (Figure 2B). This difference between the different Ub variants is not unexpected. Unlike the other residues, residue 46 is close to the so-called hydrophobic I44 patch, which plays a prominent role in the interaction of Ub

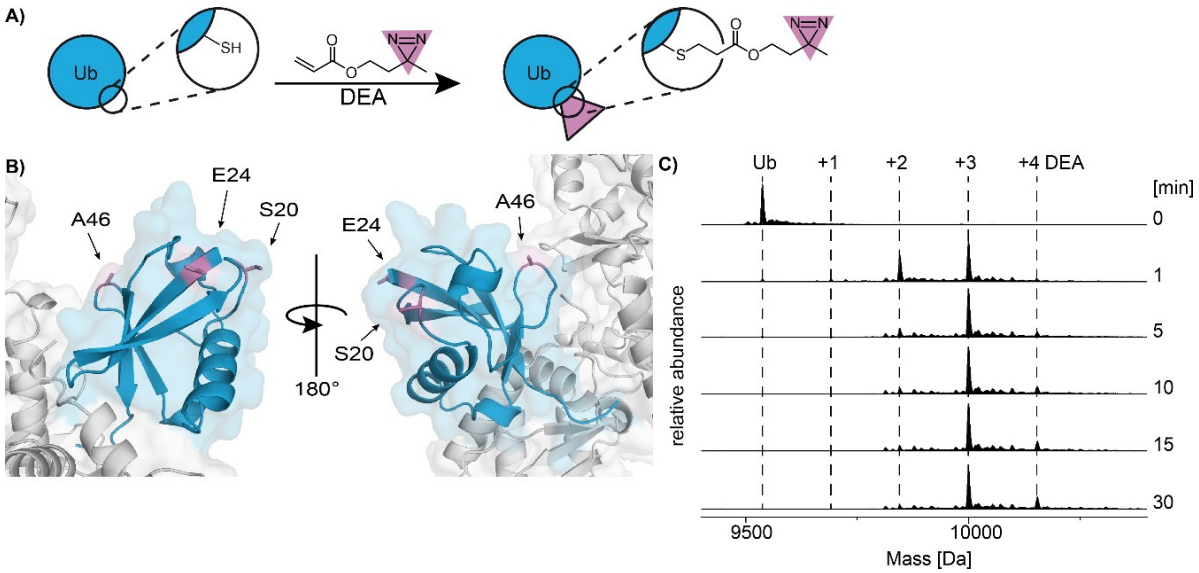

Figure 1. A) Schematic of the Michael addition used to attach DEA to genetically engineered Ub variants harboring Cys residues at distinct positions. B) AlphaFold prediction of the structure of Ub (blue) bound at the active Cys of the HECT domain of E6AP (grey). Residues (S20, E24, A46) of Ub replaced by Cys to allow Michael addition are marked in pink and the Cys side chain is represented as sticks. C) LC–MS analysis of intact Ub monitoring the labeling reaction with DEA over time. Non-modified Ub and DEA have a calculated molecular mass of 9537.8 Da and 154 Da, respectively. The calculated molecular masses of single, double, triple, and quadruple modified Ub variants are indicated

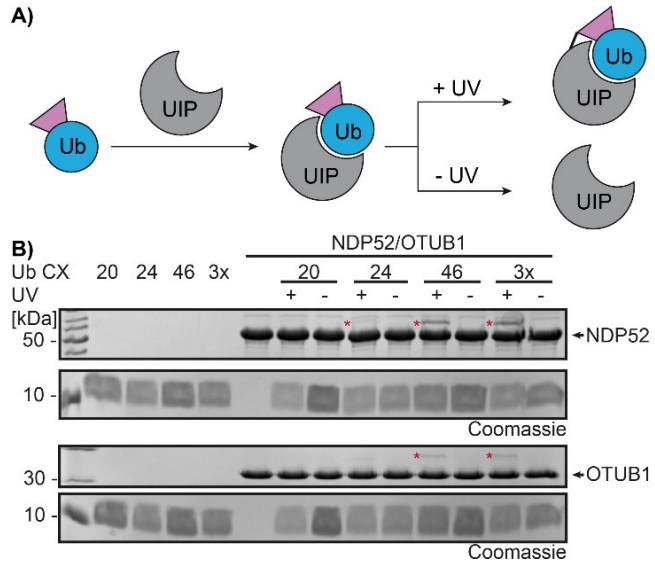

Figure 2. A) Schematic of the proof of principle photo-crosslinking reaction. DEA (pink triangle)-modified Ub is incubated with known Ub interacting proteins (UIP) and the mixture irradiated with UV light (365 nm) to induce photo-crosslinking. B) NDP52 and OTUB1 were incubated with Ub modified with DEA at position 20 (Ub C20), 24 (Ub C24), 46 (Ub C46) or at all three positions (Ub C3x) as indicated and either UV irradiated (+) or not (−). Whole reaction mixtures were separated by SDS-PAGE followed by Coomassie blue staining. Running positions of NDP52/OTUB1 crosslinked to Ub C24, Ub C46 or Ub 3DEA are indicated by an asterisk (upper panels). Lower panels show that similar amounts of Ub variants were used in each reaction.

with most known Ub binding proteins.[19] Also, the limited crosslinking efficiency with Ub C46 and Ub-3DEA is in line with the current literature, indicating that the reactive intermediates of diazirine tend to undergo reactions with any nearby molecule and thus, are likely quenched by water molecules.[20] Nevertheless, our results show that a diazirine-based Ub-photoprobe (Ub-DEA) is capable of photo-crosslinking interacting proteins and is thus suited for PCL-AE-MS assays.

Generation of a Stable Conjugate Mimicking the Intermediate E6AP-Ub Thioester Complex

As abovementioned, the formation of a thioester complex of E6AP with Ub is an essential intermediate step in E6AP-mediated ubiquitination.[2a] However, as thioester bonds are thermodynamically and kinetically rather unstable, we made use of an E6AP variant, in which the catalytic Cys residue (C820; numbering according to E6AP isoform 1)[1b] was replaced by a Lys residue (E6AP K820). The rationale for this is that K820 likely accepts activated Ub from cognate E2 enzymes by the formation of a stable isopeptide bond. In other words, Ub is trapped at the active site of E6AP and cannot be transferred to potential substrate proteins (Figure 3A). Indeed, as shown in Figure 3B, incubation of E6AP K820 with the E1 ubiquitin-activating enzyme, the E2 enzyme UbcH5b, and Ub results in the ATP-dependent formation of an E6AP molecule that according to its apparent molecular mass corresponds to mono-ubiquitinated E6AP (with a ratio of E6AP-Ub to non-modified E6AP of approximately 1 : 1). To prove that K820 is the

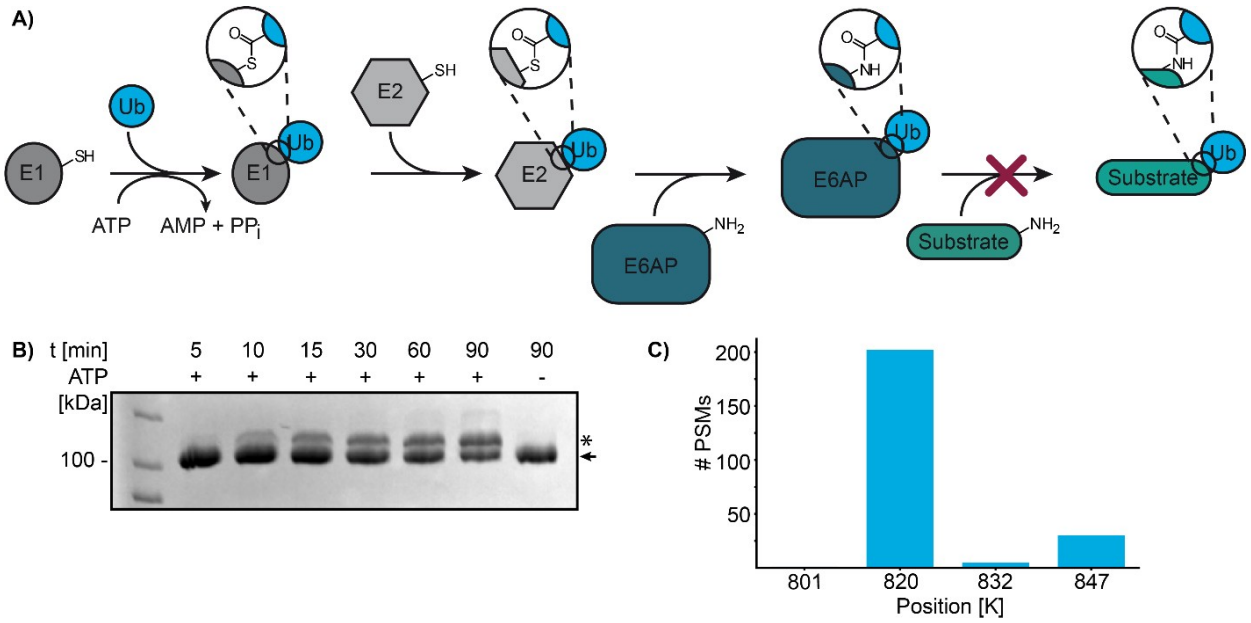

Figure 3. A) Schematic of the generation of a stable E6AP-Ub conjugate mimicking the E6AP-Ub thioester complex. E6AP K820 (substitution of the catalytic Cys residue by Lys) is incubated with the Ub-activating enzyme E1, UbcH5b (E2), and Ub in the presence of ATP. Upon E1-mediated activation of Ub, Ub is transferred from E1 to E2 via transthiolation and then from E2 to K820 of E6AP by isopeptide bond formation. In consequence, Ub cannot be passed on from E6AP to potential substrate proteins. B) The ubiquitination reaction was stopped at the indicated times and the reaction products monitored by SDS-PAGE followed by Coomassie blue staining. Reaction in the absence of ATP (−) served as negative control. Running positions of non-modified E6AP and mono-ubiquitinated E6AP are indicated by an arrowhead and asterisk, respectively. C) LC–MS/MS measurements of mono-ubiquitinated E6AP reveals K820 as primary modification site. Shown are the number of peptide spectrum matches (# PSMs) identified for the indicated positions.

main acceptor for Ub, we performed LC–MS/MS (for details, see Supporting Information). This showed that the vast majority of mono-ubiquitinated E6AP is modified at K820. As previously reported,[21] K847 was also found to be ubiquitinated, while the attachment of Ub to other Lys residues of E6AP was negligible (Figure 3C). In addition, an E6AP variant, in which Lys820 was substituted by Ala, is only poorly mono-ubiquitinated, underlining the notion that K820 represents the primary modification site (Figure S3, Supplementary Data 1).

Identification of Interaction Partners of the E6AP-Ub-3DEA Conjugate

In analogy to other enzyme-substrate interactions, it seems likely that E6AP binds only transiently to at least some of its target proteins (i.e. the K_D is rather high).[22] Thus, to increase the chances to identify such transient interactions, we generated conjugates of E6AP with Ub carrying DEA moieties at positions 20, 24, and 46 (Ub-3DEA; note that the Ub-3DEA was conjugated to E6AP K820 with an efficiency similar to wild-type Ub, FigureS4). The respective E6AP-Ub-3DEA conjugate was employed in PCL-AE-MS experiments with whole cell extracts. To do so, we equipped E6AP K820 with an N-terminal TwinStrep for immobilization on StrepTactin XT beads. Furthermore, C-terminally TwinStrep-tagged Ub-3DEA and non-modified E6AP K820 were used for comparison and empty beads as control. In brief (for a schematic workflow, see Figure 4A), the various bait molecules were incubated with whole cell extracts derived from HEK293T cells. After 3 h, PCL was performed by UV irradiation (365 nm, 2.4 J/cm^2) with the E6AP-Ub-3DEA and Ub-3DEA samples.

Subsequently, all samples were washed under mild denaturing conditions (for details, see Supporting Information), and bound proteins were eluted with biotin. The eluates were either subjected to SDS polyacrylamide gel electrophoresis (SDS-PAGE) followed by Krypton™ staining (Figure S5) or analysed by label-free quantitative MS. Significantly enriched proteins were determined by ANOVA statistics (S0 = 1; permutation-based false discovery rate (FDR) $\leq$ 0.05; for further information, see Supporting Information). After filtering for ANOVA significant hits, the results were refined by post-hoc testing via Tukey's Honestly Significant Difference (HSD) test (FDR $\leq$ 0.05). Subsequent filtering for significant pairs with E6AP-Ub-3DEA vs. the other samples (E6AP K820, Ub-3DEA, empty beads) yielded 315 significantly enriched proteins. The results were normalized over the Z-score and visualized as a heatmap after hierarchical clustering (Figure 4C). As anticipated - in part because E6AP-Ub-3DEA represents a mixture of the conjugate and non-modified E6AP (see above) and in part because many of the interactors should interact with both the E6AP-Ub conjugate and non-modified E6AP - a considerable proportion of interactors was identified with both, E6AP and E6AP-Ub-3DEA (Cluster 1, 201 proteins). A smaller fraction (Cluster 2, 57 proteins) was identified mainly with E6AP-Ub-3DEA (the full set of proteins identified is shown in Supplementary Data 2). Since these proteins were not or less efficiently enriched by Ub or non-modified E6AP K820, respectively, the respective interactions likely depend on interaction sites on both E6AP and Ub or on a distinct conformation of E6AP induced by the attachment of Ub to its catalytic site. Additional data analysis was performed by t-test (S0 = 1 and FDR = 0.05) between respective samples and are represented as volcano plots in Figure S6.

To contextualize the identified proteins, we performed functional annotation analysis using DAVID (Database for Annotation Visualization and Integrated Discovery).[23] We clustered the results with high classification stringency and the defined default annotation categories. This showed that proteins in clusters 1 and 2 can be assigned to several categories (Supplementary Data 3), with the most prominent ones presented in Figure 4C. The categories identified align well with known properties/functions of E6AP, indicating the validity of our approach. Category 1 comprises proteins that like E6AP, have been associated with neurodevelopmental disorders.[24] The ability of E6AP to interact with the 26S proteasome is well established[8a,25] and accordingly, various subunits of the proteasome are represented in category 2. Similarly, it was previously reported that E6AP interacts with ribosomal proteins (category 3)[26] and that it affects the structural stability of neurons (category 4).[27] Finally, category 5 comprises proteins involved in oxidative phosphorylation. Notably, there is evidence that Dup15q individuals, which overexpress E6AP, suffer from mitochondrial dysfunction.[28] Moreover, results obtained with mitochondria derived from the brain of AS model mice indicate that loss of E6AP also correlates with mitochondrial dysfunction and in addition with impaired morphology of the mitochondrial inner membrane and reduced oxidative phosphorylation.[29] Finally, E6AP has been found at the mitochondrial outer membrane,[30] and transcriptomic analyses link E6AP to the regulation of mitochondrial function and the production of radical oxygen species (ROS).[31]

Besides the correlations on the cellular pathway/process level, we identified several known interactors of E6AP (Figure 5A). HERC2, a member of the HECT E3 family that has been causally associated with an AS-related neurodevelopmental disorder,[32] and NEURL4 were previously found together with E6AP in a high molecular mass complex referred to as the HUN complex (HERC2, UBE3A and NEURL4).[8a] Moreover, we previously identified HERC2 as an activator of E6AP.[13] While HERC2 and NEURL4 may not represent substrates of E6AP, MCM7, which is involved in DNA replication, and the proteasomal subunit PSMD4, also known as RPN10, have been reported to be substrates of E6AP.[33] HERC2, NEURL4, MCM7, and PSMD4/RPN10 were enriched with both E6AP-Ub-3DEA and non-modified E6AP, indicating that their interaction is only mildly influenced by the Ub-loading status of E6AP (see Figure S6 for a direct comparison of proteins enriched by E6AP-Ub-3DEA and non-modified E6AP). MSH2, a key player in DNA mismatch repair, was also slightly enriched in E6AP-Ub-3DEA samples compared to E6AP alone (Figure 5A, Figure S6B). As a connection between MSH2 and E6AP has not been reported so far, we performed an in vitro ubiquitination assay. This showed that E6AP indeed facilitates ubiquitination of MSH2 (Figure 5B). This suggests a potential role for E6AP in regulating DNA mismatch

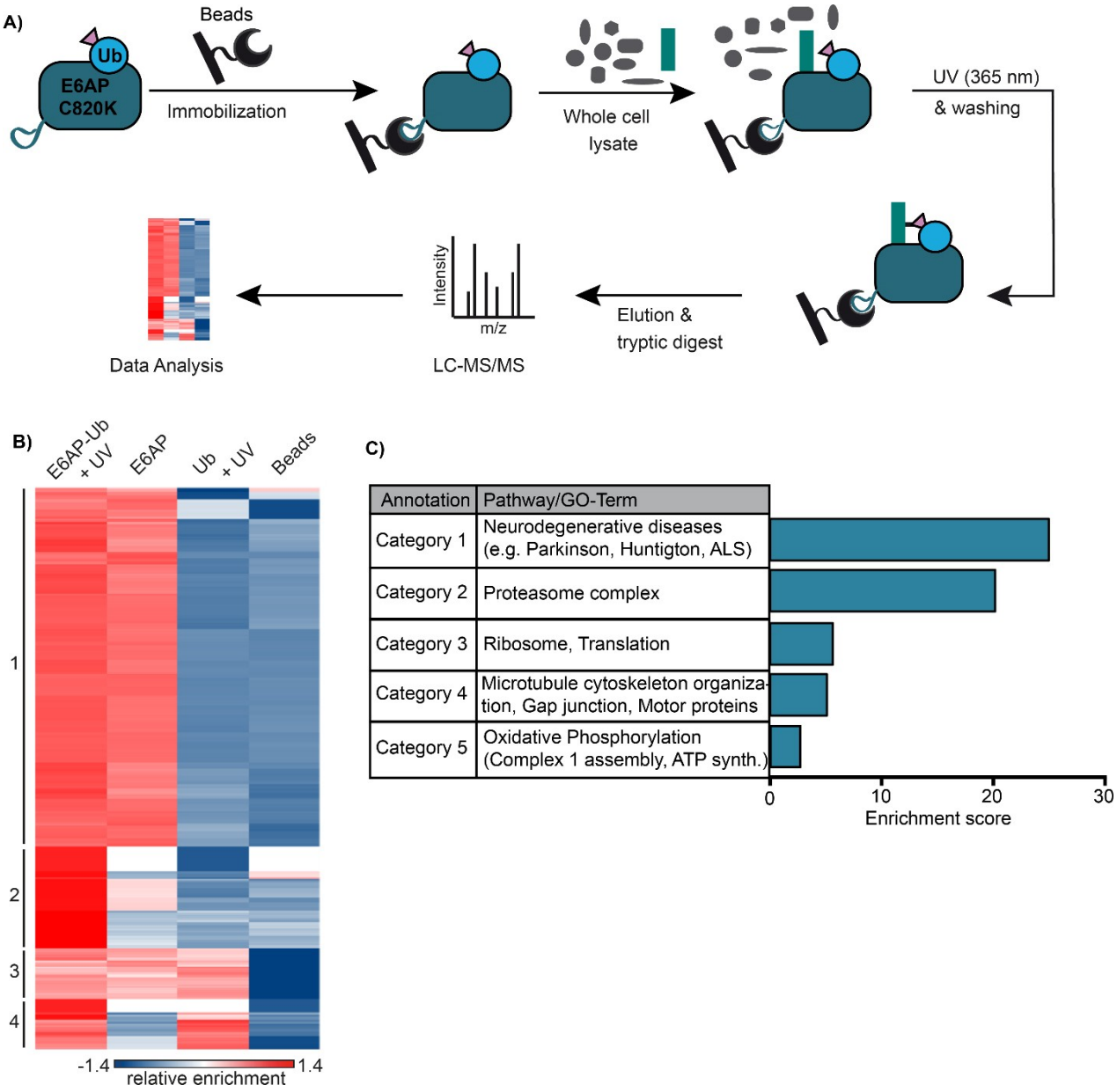

Figure 4. A) Schematic overview of the of the PCL-AE-MS workflow for the identification of interactors of E6AP-Ub-3DEA. E6AP-Ub-3DEA (E6AP-Ub), non-modified E6AP, Ub-3DEA (Ub) were used as bait molecules for affinity enrichment and incubated with HEK293T cell extract. Empty beads were used as control. B) Hierarchical clustering of statistically significant interactors (rows) of the different bait molecules (columns). Red indicates enrichment, whereas blue indicates lack of enrichment. Thresholds for ANOVA statistics were set to FDR $\leq$ 0.05 and S0 = 1. Cluster numbers are indicated on the left. Note that Cluster 2 contains 57 proteins that are preferentially enriched by E6AP-Ub; only 4 of these (UCHL5, UBR5, UBAC2, WRNIP1) contain known Ub-binding domains. C) Functional annotation analysis of clusters 1 and 2 using DAVID (Database for Annotation, Visualization and Integrated Discovery).[23]

repair processes, a proposition that needs to be confirmed in future studies.

In contrast to the abovementioned proteins, DDX3X and UCHL5, also known as UCH37, were preferentially enriched with E6AP-Ub-3DEA (Figure 5A). DDX3X was previously identified by us as a potential substrate of the HPV E6 oncoprotein in complex with E6AP.[34] In support of the present data, we also reported that E6AP ubiquitinates DDX3X in vitro in the absence of E6, though with reduced efficiency[34]. UCHL5 was identified as a potential substrate of Drosophila E6AP[33b] and of human E6AP in context of the interaction of E6AP with the 26S proteasome.[35] To confirm that UCHL5 preferentially interacts with E6AP, when it is loaded with Ub, we performed coprecipitation experiments with in vitro translated radioactively labelled UCHL5 and our TwinStrep-tagged versions of non-modified E6AP and E6AP-Ub-3DEA (Figure 5B). The results obtained show that UCHL5 preferentially interacts with E6AP-Ub-3DEA, indicating the usefulness of our PCL-AE-MS approach. Finally, UCHL5 is in vitro efficiently ubiquitinated by E6AP (Figure 5D), even in the absence of the HPV E6 oncoprotein, supporting the notion that UCHL5 is a substrate of E6AP of potential relevance for E6AP-associated disorders.

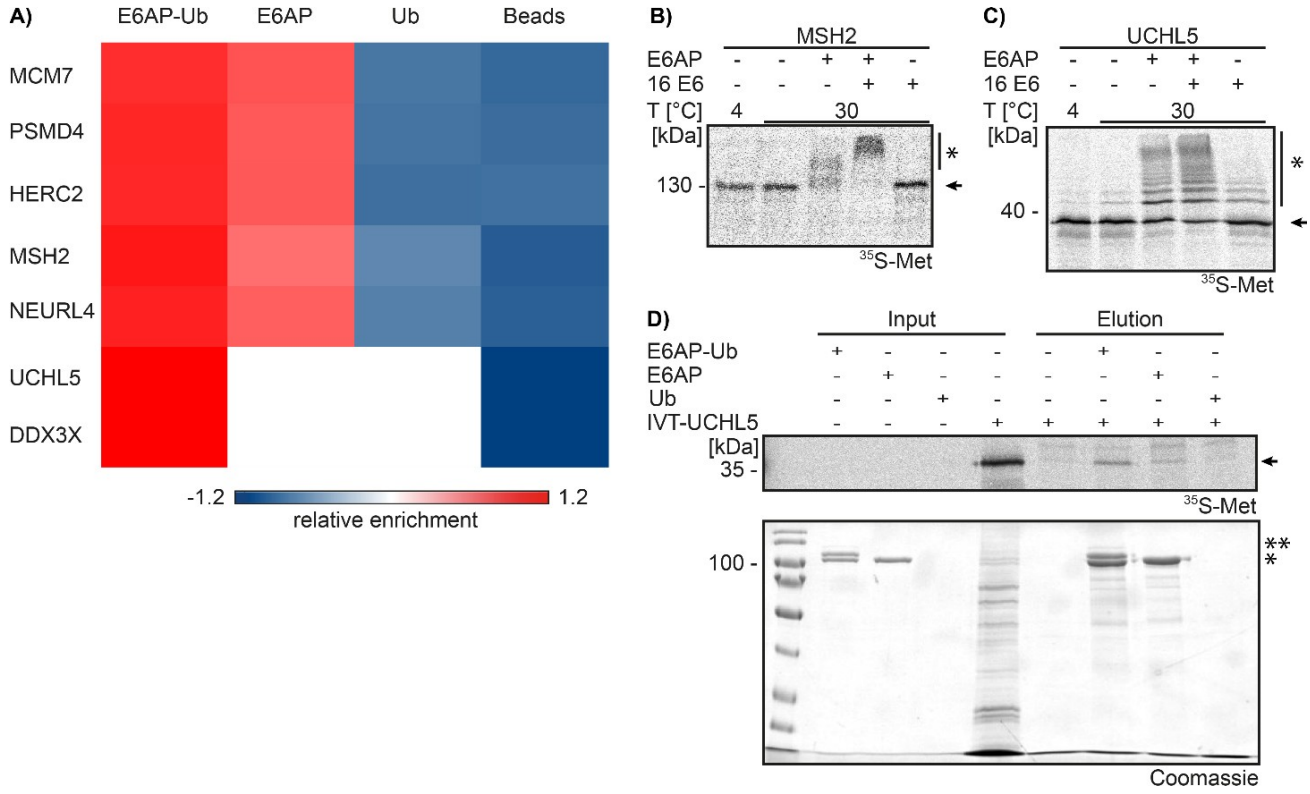

Figure 5. A) Selected interactors of E6AP-Ub-3DEA (E6AP-Ub) and non-modified E6AP (E6AP). Red indicates enrichment, whereas blue indicates lack of enrichment. B) and C) In vitro ubiquitination reactions with in vitro translated radiolabeled MSH2 (B) and UCHL5 (C) were performed as described in Supporting Information in the presence or absence of E6AP and the HPV E6 oncoprotein at 30 °C as indicated. Reaction at 4 °C served as negative control. After 60 min, reactions were stopped and analyzed by SDS-PAGE followed by fluorography. Running positions of non-modified MSH2/UCHL5 and ubiquitinated forms of MSH2/UCHL5 are indicated by an arrowhead and an asterisk, respectively. D) In vitro binding assay using in vitro translated radiolabelled UCHL5 and Strep-tagged versions of E6AP-Ub-3DEA (E6AP-Ub), non-modified E6AP (E6AP), Ub-3DEA (Ub), and empty beads as affinity matrices as indicated. Binding reactions (Elution) were analyzed by SDS-PAGE followed by fluorography to visualize UCHL5 (upper panel, marked by an arrowhead) or by Coomassie blue staining (lower panel). Input, 10% of the proteins used in the binding assays. Running positions of non-modified E6AP and E6AP-Ub are marked with one asterisk or two asterisks, respectively.

Conclusions

Dysregulation of the Ub ligase activity of E6AP has been associated with the development of cervical cancer, AS, and the Dup15q syndrome. To understand how dysregulation of E6AP contributes to these disorders and to eventually come up with new treatment strategies, it is important to elucidate the cellular pathways/processes that are controlled by E6AP and, thus, its substrates. Here, we employed a stable E6AP-Ub conjugate as a surrogate for the kinetically unstable E6AP-Ub thioester complex, which represents an essential intermediate in E6AP-mediated ubiquitination[2a] and, thus, the most suitable affinity matrix for substrate identification. In addition, since at least in some cases, the interaction of E6AP with its substrates may be rather transient, a Ub variant was designed that harbors a photo-reactive probe (DEA) at distinct positions to allow covalent trapping of potential substrate proteins. Our proof-of-principle PCL-AE-MS experiments revealed overlapping, yet distinct enrichment patterns for E6AP-Ub-3DEA and non-modified E6AP (Figure 4B, Figure S6B), supporting our proposition that E6AP-Ub conjugates are the matrix of choice for identifying substrates of E6AP. Due to the rather low PCL efficiency of Ub-3DEA (Figure 2), it seems likely that we were not able to enrich and identify all of the substrates that only transiently interact with E6AP. Although we deliberately employed Ub-3DEA harboring three DEA moieties at different positions of Ub, we cannot exclude that the low PCL efficiency is in part explained by the notion that the positions we chose for DEA placement, which has been reported to be critical for PCL efficiency,[36] were not ideal. Irrespective of this possibility, in the future it will be important to develop more efficient PCL probes. Finally, Ub thioester complexes are essential intermediates in the final attachment of Ub to any substrate protein, regardless if the attachment is catalyzed by E3 enzymes, as in the case of E6AP, or by E2 enzymes, as in the case of RING E3 ligases.[3] Based on this shared mechanism, we suggest that stable enzyme-Ub conjugates mimicking the respective enzyme-Ub thioester complex in combination with PCL are generally suited to identify substrate proteins of distinct E2 and E3 enzymes. Future studies will show if this proposition holds true.

Supporting Information

The authors have cited additional references within the Supporting Information.[16,37]

Acknowledgements

We thank Dr. Andreas Marquardt and Dr. Anna Sladewska-Marquardt of the Proteomics Center of the University of Konstanz for assistance with mass spectrometric experiments. We gratefully acknowledge funding by the Deutsche Forschungsgemeinschaft (SFB 969, project B03) and financial support by the Konstanz Research School Chemical Biology. Open Access funding enabled and organized by Projekt DEAL.

Conflict of Interests

The authors declare no conflict of interest.

Data Availability Statement

The mass spectrometry proteomics data have been deposited to the ProteomeXchange Consortium via the PRIDE partner repository with the dataset identifier PXD055649. (Username: reviewer pxd055649@ebi.ac.uk; Password: VDaeLaQm6CX8).

Keywords: E6AP/UBE3A · ubiquitination · photoaffinity labeling · proteomics · substrate identification

[1] a) J. S. Sutcliffe, Y. H. Jiang, R. J. Galijaard, T. Matsuura, P. Fang, T. Kubota, S. L. Christian, J. Bressler, B. Cattanach, D. H. Ledbetter, A. L. Beaudet, *Genome Res.* **1997**, *7*, 368–377; b) Y. Yamamoto, J. M. Huibregtse, P. M. Howley, *Genomics* **1997**, *41*, 263–266.
[2] a) M. Scheffner, U. Nuber, J. M. Huibregtse, *Nature* **1995**, *373*, 81–83; b) J. M. Huibregtse, M. Scheffner, S. Beaudenon, P. M. Howley, *Proc. Natl. Acad. Sci. USA* **1995**, *92*, 2563–2567.
[3] N. Zheng, N. Shabek, *Annu. Rev. Biochem.* **2017**, *86*, 129–157.
[4] S. Beaudenon, J. M. Huibregtse, *BMC Biochem.* **2008**, *9 Suppl. 1*, S4.
[5] a) T. Kishino, M. Lalande, J. Wagstaff, *Nat. Genet.* **1997**, *15*, 70–73; b) T. Matsuura, J. S. Sutcliffe, P. Fang, R. J. Galjaard, Y. H. Jiang, C. S. Benton, J. M. Rommens, A. L. Beaudet, *Nat. Genet.* **1997**, *15*, 74–77; c) J. T. Glessner, K. Wang, G. Cai, O. Korvatska, C. E. Kim, S. Wood, H. Zhang, A. Estes, C. W. Brune, J. P. Bradfield, M. Imielinski, E. C. Frackelton, J. Reichert, E. L. Crawford, J. Munson, P. M. Sleiman, R. Chiavacci, K. Annaiah, K. Thomas, C. Hou, W. Glaberson, J. Flory, F. Otieno, M. Garris, L. Soorya, L. Klei, J. Piven, K. J. Meyer, E. Anagnostou, T. Sakurai, R. M. Game, D. S. Rudd, D. Zurawiecki, C. J. McDougle, L. K. Davis, J. Miller, D. J. Posey, S. Michaels, A. Kolevzon, J. M. Silverman, R. Bernier, S. E. Levy, R. T. Schultz, G. Dawson, T. Owley, W. M. McMahon, T. H. Wassink, J. A. Sweeney, J. I. Nurnberger, H. Coon, J. S. Sutcliffe, N. J. Minshew, S. F. Grant, M. Bucan, E. H. Cook, J. D. Buxbaum, B. Devlin, G. D. Schellenberg, H. Hakonarson, *Nature* **2009**, *459*, 569–573; d) A. Hogart, D. Wu, J. M. LaSalle, N. C. Schanen, *Neurobiol. Dis.* **2010**, *38*, 181–191; e) K. Buiting, C. Williams, B. Horsthemke, *Nat. Rev. Neurol.* **2016**, *12*, 584–593.
[6] A. Owais, R. K. Mishra, H. Kiyokawa, *Cancers* **2020**, *12*, 2108.
[7] J. C. Krzeski, M. C. Judson, B. D. Philpot, *Curr. Opin. Neurobiol.* **2024**, *88*, 102899.
[8] a) G. Martinez-Noel, J. T. Galligan, M. E. Sowa, V. Arndt, T. M. Overton, J. W. Harper, P. M. Howley, *Mol. Cell. Biol.* **2012**, *32*, 3095–3106; b) T. Shimoji, K. Murakami, Y. Sugiyama, M. Matsuda, S. Inubushi, J. Nasu, M. Shirakura, T. Suzuki, T. Wakita, T. Kishino, H. Hotta, T. Miyamura, I. Shoji, *J. Cell. Biochem.* **2009**, *106*, 1123–1135.
[9] N. J. Pandya, S. Meier, S. Tyanova, M. Terrigno, C. Wang, A. M. Punt, E. J. Mientjes, A. Vautheny, B. Distel, T. Kremer, Y. Elgersma, R. Jagasia, *Mol. Psychiatry* **2022**, *27*, 2590–2601.
[10] Y. Wang, X. Liu, L. Zhou, D. Duong, K. Bhuripanyo, B. Zhao, H. Zhou, R. Liu, Y. Bi, H. Kiyokawa, J. Yin, *Nat. Commun.* **2017**, *8*, 2232.
[11] S. Kumar, A. L. Talis, P. M. Howley, *J. Biol. Chem.* **1999**, *274*, 18785–18792.
[12] D. Zaaroor-Regev, P. de Bie, M. Scheffner, T. Noy, R. Shemer, M. Heled, I. Stein, E. Pikarsky, A. Ciechanover, *Proc. Natl. Acad. Sci. USA* **2010**, *107*, 6788–6793.
[13] S. Kühnle, U. Kogel, S. Glockzin, A. Marquardt, A. Ciechanover, K. Matentzoglu, M. Scheffner, *J. Biol. Chem.* **2011**, *286*, 19410–19416.
[14] Z. Wang, F. Fan, Z. Li, F. Ye, Q. Wang, R. Gao, J. Qiu, Y. Lv, M. Lin, W. Xu, *Nat. Commun.* **2024**, *15*, 3531.
[15] a) J. Jumper, R. Evans, A. Pritzel, T. Green, M. Figurnov, O. Ronneberger, K. Tunyasuvunakool, R. Bates, A. Zidek, A. Potapenko, A. Bridgland, C. Meyer, S. A. A. Kohl, A. J. Ballard, A. Cowie, B. Romera-Paredes, S. Nikolov, R. Jain, J. Adler, T. Back, S. Petersen, D. Reiman, E. Clancy, M. Zielinski, M. Steinegger, M. Pacholska, T. Berghammer, S. Bodenstein, D. Silver, O. Vinyals, A. W. Senior, K. Kavukcuoglu, P. Kohli, D. Hassabis, *Nature* **2021**, *596*, 583–589; b) M. Varadi, S. Anyango, M. Deshpande, S. Nair, C. Natassia, G. Yordanova, D. Yuan, O. Stroe, G. Wood, A. Laydon, A. Zidek, T. Green, K. Tunyasuvunakool, S. Petersen, J. Jumper, E. Clancy, R. Green, A. Vora, M. Lutfi, M. Figurnov, A. Cowie, N. Hobbs, P. Kohli, G. Kleywegt, E. Birney, D. Hassabis, S. Velankar, *Nucleic Acids Res.* **2022**, *50*, D439–D444.
[16] C. Chou, R. Uprety, L. Davis, J. W. Chin, A. Deiters, *Chem. Sci.* **2011**, *2*, 480–483.
[17] X. Zhao, J. Lutz, E. Höllmüller, M. Scheffner, A. Marx, F. Stengel, *Angew. Chem. Int. Ed. Engl.* **2017**, *56*, 15764–15768.
[18] a) Q. Deveraux, C. Jensen, M. Rechsteiner, *J. Biol. Chem.* **1995**, *270*, 23726–23729; b) T. L. Thurston, G. Ryzhakov, S. Bloor, N. von Muhlinen, F. Randow, *Nat. Immunol.* **2009**, *10*, 1215–1221; c) T. Wang, L. Yin, E. M. Cooper, M. Y. Lai, S. Dickey, C. M. Pickart, D. Fushman, K. D. Wilkinson, R. E. Cohen, C. Wolberger, *J. Mol. Biol.* **2009**, *386*, 1011–1023.
[19] I. Dikic, S. Wakatsuki, K. J. Walters, *Nat. Rev. Mol. Cell Biol.* **2009**, *10*, 659–671.
[20] J. Wang, J. Kubicki, H. Peng, M. S. Platz, *J. Am. Chem. Soc.* **2008**, *130*, 6604–6609.
[21] F. Mortensen, D. Schneider, T. Barbic, A. Sladewska-Marquardt, S. Kühnle, A. Marx, M. Scheffner, *Proc. Natl. Acad. Sci. USA* **2015**, *112*, 9872–9877.
[22] N. W. Pierce, G. Kleiger, S. O. Shan, R. J. Deshaies, *Nature* **2009**, *462*, 615–619.
[23] W. Huang da, B. T. Sherman, R. A. Lempicki, *Nat. Protoc.* **2009**, *4*, 44–57.
[24] S. J. Lopez, D. J. Segal, J. M. LaSalle, *Front. Mol. Neurosci.* **2019**, *11*, 476.
[25] G. R. Buel, X. Chen, R. Chari, M. J. O'Neill, D. L. Ebelle, C. Jenkins, V. Sridharan, S. G. Tarasov, N. I. Tarasova, T. Andresson, K. J. Walters, *Nat. Commun.* **2020**, *11*, 1291.
[26] G. Martinez-Noel, K. Luck, S. Kuhnle, A. Desbuleux, P. Szajner, J. T. Galligan, D. Rodriguez, L. Zheng, K. Boyland, F. Leclere, Q. Zhong, D. E. Hill, M. Vidal, P. M. Howley, *J. Mol. Biol.* **2018**, *430*, 1024–1050.
[27] N. Khatri, J. P. Gilbert, Y. Huo, R. Sharaflari, M. Nee, H. Qiao, H. Y. Man, *J. Neurosci.* **2018**, *38*, 363–378.
[28] P. A. Filipek, J. Juranek, M. Smith, L. Z. Mays, E. R. Ramos, M. Bocian, D. Masser-Frye, T. M. Laulhere, C. Modahl, M. A. Spence, J. J. Gargus, *Ann. Neurol.* **2003**, *53*, 801–804.
[29] H. Su, W. Fan, P. E. Coskun, J. Vesa, J. A. Gold, Y. H. Jiang, P. Potluri, V. Procaccio, A. Acab, J. H. Weiss, D. C. Wallace, V. E. Kimonis, *Neurosci. Lett.* **2011**, *487*, 129–133.
[30] A. C. Burette, M. C. Judson, A. N. Li, E. F. Chang, W. W. Seeley, B. D. Philpot, R. J. Weinberg, *Mol. Autism* **2018**, *9*, 54.
[31] J. Panov, L. Simchi, Y. Feuermann, H. Kaphzan, *Int. J. Mol. Sci.* **2020**, *21*, 4156.
[32] G. V. Harlalka, E. L. Baple, H. Cross, S. Kuhnle, M. Cubillos-Rojas, K. Matentzoglu, M. A. Patton, K. Wagner, R. Coblentz, D. L. Ford, D. J. Mackay, B. A. Chioza, M. Scheffner, J. L. Rosa, A. H. Crosby, *J. Med. Genet.* **2013**, *50*, 65–73.
[33] a) C. Kühne, L. Banks, *J. Biol. Chem.* **1998**, *273*, 34302–34309; b) S. Y. Lee, J. Ramirez, M. Franco, B. Lectez, M. Gonzalez, R. Barrio, U. Mayor, *Cell. Mol. Life Sci.* **2014**, *71*, 2747–2758.
[34] F. A. Ebner, C. Sailer, D. Eichbichler, J. Jansen, A. Sladewska-Marquardt, F. Stengel, M. Scheffner, *J. Biol. Chem.* **2020**, *295*, 15070–15082.

[35] A. D. Jacobson, A. MacFadden, Z. Wu, J. Peng, C. W. Liu, *Mol. Biol. Cell* **2014**, *25*, 1824–1835.
[36] T. Yang, Z. Liu, X. D. Li, *Chem. Sci.* **2015**, *6*, 1011–1017.
[37] a) K. Stuber, T. Schneider, J. Werner, M. Kovermann, A. Marx, M. Scheffner, *Nat. Commun.* **2021**, *12*, 5939; b) A. Shevchenko, H. Tomas, J. Havlis, J. V. Olsen, M. Mann, *Nat. Protoc.* **2006**, *1*, 2856–2860; c) J. Cox, M. Y. Hein, C. A. Luber, I. Paron, N. Nagaraj, M. Mann, *Mol. Cell. Proteomics* **2014**, *13*, 2513–2526; d) J. Cox, M. Mann, *Nat. Biotechnol.* **2008**, *26*, 1367–1372; e) S. Tyanova, T. Temu, P. Sinitcyn, A. Carlson, M. Y. Hein, T. Geiger, M. Mann, J. Cox, *Nat. Methods* **2016**, *13*, 731–740; f) Y. Perez-Riverol, J. Bai, C. Bandla, D. García-Seisdedos, S. Hewapathirana, S. Kamatchinathan, D. J. Kundu, A. Prakash, A. Frericks-Zipper, M. Eisenacher, *Nucleic Acids Res.* **2022**, *50*, D543–D552; g) F. Offensperger, F. Müller, J. Jansen, D. Hammler, K. H. Götz, A. Marx, C. L. Sirois, S. J. Chamberlain, F. Stengel, M. Scheffner, *Cell Chem. Biol.* **2020**, *27*, 1510–1520.

Manuscript received: October 8, 2024
Revised manuscript received: January 2, 2025
Accepted manuscript online: January 11, 2025
Version of record online: January 23, 2025